Influence of Local Ensemble Transform Kalman Filter with the NICAM on High Latitudes

Keiichi KONDO [1] and Hiroshi L. TANAK A[2]

1: Life and Environmental Sciences, University of Tsukuba, Japan

2: Center for Computational Sciences, University of Tsukuba, Japan

1. INTRODUCTION

Data assimilation is one of the most important techniques in numerical weather predictions. In some operational centers, 4D-Var (e.g., H. Liu and X. Zou 2001, and Pierre and Jean-Noël 2001) has been used recently, but many operational centers use 3D-Var (Parrish and Derber 1992), which is an economical and accurate statistical interpolation scheme. The 4D-Var's accuracy is much higher than the 3D-Var. In addition to 4D-Var's high accuracy, it allows the assimilation of many observations, for example asynchronous observations such as satellite radiances, at their correct observation time. However, the computational cost of the 4D-Var implementation is very expensive because the 4D-Var requires a linear tangent model and its adjoint model.

Evensen (1994) suggested an ensemble Kalman filter (hereafter EnKF), which approximates the covariance matrix of the Kalman filter (Kalman 1960) using ensemble predictions. The EnKF does not require calculation of a linear tangent model and its adjoint model of GCMs. They have very large degrees of freedom, so the KF requires very large covariance matrices, but the EnKF does not require computing the covariance matrices, directly. Moreover, The EnKF is able to generate the optimum ensemble perturbations which reflect analysis error.

Local ensemble transform Kalman filter (Hunt et al. 2007, hereafter LETKF) is a kind of EnKFs. In the LETKF each grid point has a local patch. The LETKF has an important advantage in which the observations are assimilated in each local patch. Because of this advantage, the LETKF has a higher performance to implement in parallel computers. Miyoshi et al. (2007a) applied the LETKF to AFES with a T159L48 resolution to perform an experimental reanalysis and investigated the stability of the LETKF. Miyoshi et al. (2007b) constructed LETKF without the local patch, and the non-local patch LETKF improves analysis errors in polar region.

There have been a few researches applying EnKF to nonhydrostatic models. Snyder and Zhang (2003) applied an ensemble square root filter (EnSRF, Whitaker and Hamill 2002) which is a kind of EnKFs. Miyoshi and Aranami (2006) applied the LETKF to JMA's operational version of NHM.

On the other hand, NICAM (Nonhydrostatic ICosahedral Atmospheric Model, Sato et al. 2008) is a nonhydrostatic global atmospheric model. It adopted the nonhydrostatic equations and icosahedral grid structure. So, the NICAM can calculate convection directly. The NICAM is developed to resolve clouds, and has high performance in the case of high parallel computing. It is expected to understand the rainfall system more. However, assimilation system of the NICAM has not been constructed. So in this study, we apply non-local patch version of the LETKF to the NICAM (NICAM-LETKF), and investigate the influence of the NICAM-LETKF in high latitudes under perfect model assumption.

2. EXPERIMENTAL SETTINGS

Two kinds of experiments (hereafter Ex1 and Ex2) are performed under the perfect model assumption in this study. In the Ex1, observing elements are pressure, temperature and wind components. In the Ex2 observing elements are the elements of Ex1 and mixing ratio of water vapor.

The forecast model is the abovementioned

NICAM. Its horizontal resolution is 224 km (Glevel-5) and the number of vertical layers is 40. The prognostic variables are pressure, temperature, horizontal wind component, vertical wind and mixing ratio of water vapor, cloud water and rain water. The true control run is generated with an initial data by the JMA-GSM analysis on 12Z December 29 2006, and integrated until 12Z January 15 2007. Observations are generated by adding simulated observational error. The error standard deviations are 1.0 hPa (pressure), 1.0 K (temperature), 1.0 m/s (horizontal wind) and 0.5 g/kg (mixing ratio of water vapor). The observational density is about 4% of 3-dimensional space out of the enter grid.

In this study, the localization of the LETKF adopts Gaussian-like fifth function. The localization scale is defined as 1 standard deviation. The horizontal localization scale is 300 km, and vertical localization scale is 1.5-grid. The Gaussian-like function drops to 0 at about 1095 km and 6.7 vertical grids. The NICAM-LETKF assimilation cycle is every 6 hours, and the assimilation term is 10 days. The period of the experimental assimilation is from 12Z 1 January 2007 to 12Z 15 January 2007. The ensemble size is chosen to be 20, and the 4% (Ex1) and 3% (Ex2) multiplicative spread inflation are employed.

3. RESULTS

Figure 1 and Figure 2 respectively show the time series of analysis root mean square errors (RMSEs)

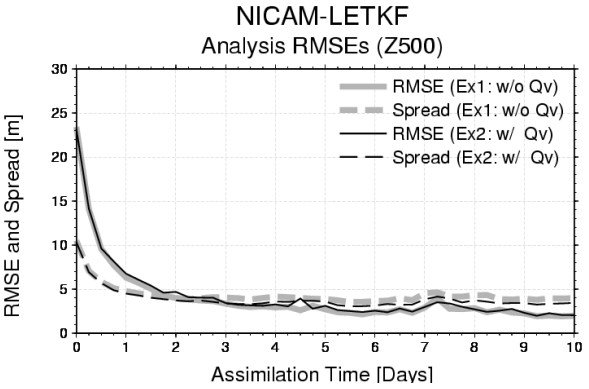

Fig. 1. The time series of the analysis RMSEs and ensemble spreads for 500 hPa geopotential height (m). Initial time is 12Z 6 Jan 2007.

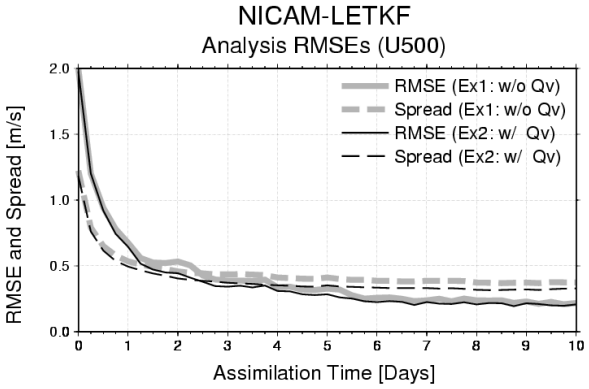

Fig. 2. As in Fig. 1, but for the time series of the analysis RMSEs and ensemble spreads for 500 hPa zonal wind (m/s).

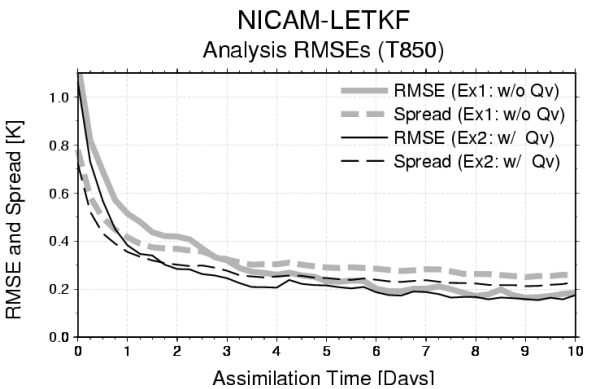

Fig. 3. As in Fig. 1, but for the time series of the analysis RMSEs and ensemble spreads for 850 hPa temperature (K).

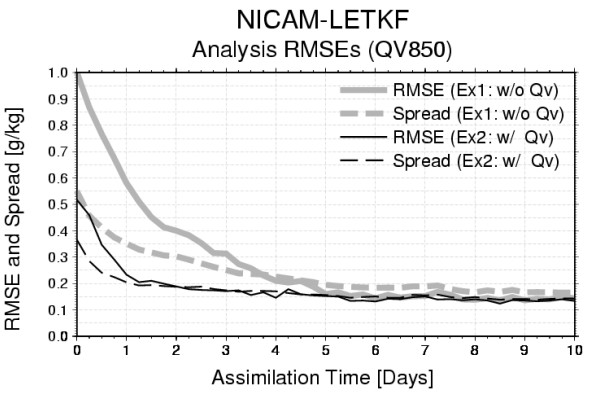

Fig. 4. As in Fig. 1, but for the time series of the analysis RMSEs and ensemble spreads for 850 hPa mixing ratio of water vapor (g/kg).

and ensemble spreads in the Northern Hemisphere (20° N - 90° N) for 500 hPa geopotential height and zonal wind. In early period the RMSEs decrease with time, and the RMSEs are smaller than the observational errors. The NICAM-LETKF is slightly larger than the RMSEs due to the 3 or 4% spread inflation. However, it is said that the ensemble spreads roughly correspond to the RMSEs, so the NICAM-LETKF captures analysis error in the Northern Hemisphere. Comparing Ex1 and Ex2, it is seen that the RMSEs of the Ex1 and Ex2 are almost the same during the experimental period in Fig. 1 and Fig. 2. It suggests that the impact of assimilating water vapor is not so large.

Figure 3 and Figure 4 show the time series of analysis RMSEs and ensemble spreads in the Northern Hemisphere for 850 hPa temperature and mixing ratio of water vapor, respectively. As in Fig. 1 and Fig. 2, in early period the RMSEs degrease with time, and the RMSEs are smaller than the observational errors. In early period the RMSE of Ex1 is larger than that of Ex2. However, in the latter half of the period, the RMSE of Ex1 becomes comparable to that of Ex2. This suggests that in early period assimilating water vapor influences the RMSE of the EX1. The EnKF is able to treat the cross-covariance structure among different variables. So in the latter half of the period, the field of water vapor is improved by assimilating other observational elements which are related to the water vapor.

Figure 5 shows the spatial distribution of the analysis RMSE (top panel) and ensemble spread (bottom panel) for 500 hPa geopotential height (left panel) and zonal wind (right panel) about Ex2 on 18Z 8 January 2007. Shaded area shows the analysis RMSE and ensemble spread, and the contours show 500 hPa geopotential height. In the field of geopotential height (left panel), there is a developed low in Kamchatka. In the east of the low, the RMSE is large, but the ensemble spread is as large as the RMSE. So the NICAM-LETKF is able to capture regional analysis errors in middle troposphere. In the field of zonal wind (right panel), in the dense region of the contour, the RMSE and ensemble spread are large, so it represents that the RMSE and ensemble spread become large in high chaotic area.

Figure 6 shows the spatial distribution of the analysis RMSE (top panel) and ensemble spread (bottom panel) for 850 hPa temperature (left panel) and mixing ratio of water vapor (right panel) about

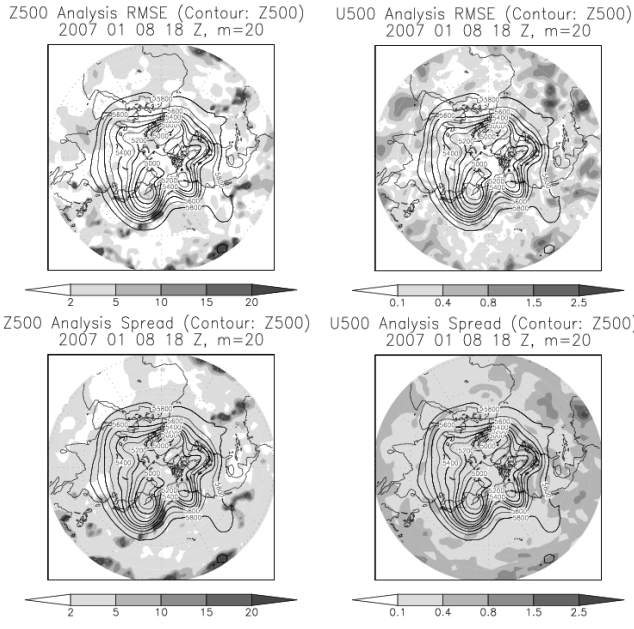

Fig. 5. The spatial distributions of the analysis RMSEs (top panel) and ensemble spreads (bottom panel) for 500 hPa geopotential height (left panel) and zonal wind (right panel).

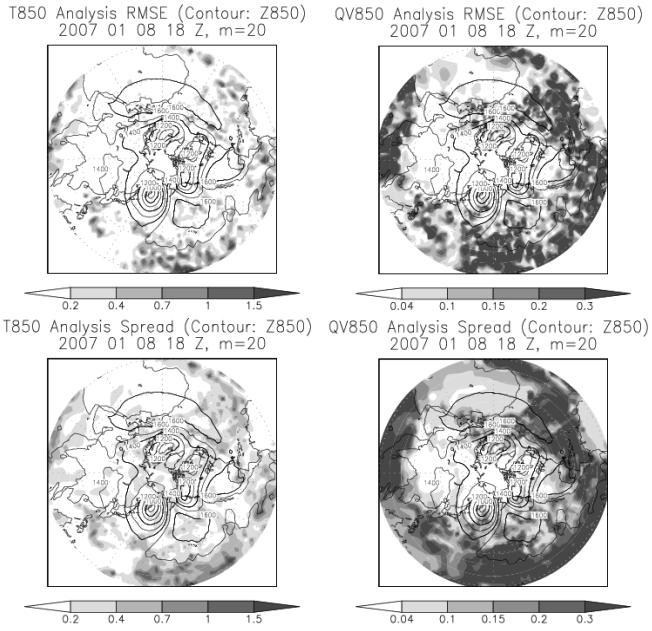

Fig. 6. The spatial distributions of the analysis RMSEs (top panel) and ensemble spreads (bottom panel) for 850 hPa temperature (left panel) and mixing ratio of water vapor (right panel).

Ex2 on 18Z 8 January 2007. In the fields of temperature and water vapor, the RMSEs and ensemble spreads show good correspondence. The areas of large RMSE correspond to the ocean. Because the water vapor is supplied from the ocean, the areas over the ocean become highly chaotic. So in the temperature and water vapor fields, the RMSEs become large. However, the ensemble spreads are large in such areas. This suggests that the NICAM-LETKF is able to capture the regional analysis errors in lower troposphere. In Fig. 5 and Fig. 6, the area which the RMSE and ensemble spread are large is not seen in the high latitudes. In the case of Ex1, the similar results are provided (not shown).

4. CONCLUSION and DISCUSSION

In this study, the LETKF has been applied and tested with the NICAM. For the first part, it is confirmed that the LETKF works appropriately with a nonhydrostatic global model. It is seen that the NICAM-LETKF works stably even if the ensemble size is 20 without assimilating water vapor. In early assimilation period, the positive impact of assimilating water vapor appears in the fields of temperature and water vapor. In the latter half of the period, the analysis RMSEs of Ex1 corresponds to that of Ex2. EnKF computes error covariance explicitly. So, the EnKF is able to treat the cross-covariance structure. The structure explains the dynamical balance among different variables. Therefore, it is consider that the EnKF does not require an initialization process. Actually, Miyoshi and Yamane (2007) confirmed that the localization does not destroy the cross-covariance structure completely, and the LETKF works very stably even if the forecast model comparatively has high resolution. On the other hand, in the fields of geopotential height and zonal wind, the positive impact appears slightly.

For the second part, it is confirmed that the NICAM-LETKF can capture the high chaotic area, for example the east of the developed low and over the ocean, by investigating the correspondence of the spatial distribution of RMSEs and ensemble spread. However, it is necessary to investigate the case of high chaotic phenomena such as blocking in detail, because in this assimilation period the RMSEs and ensemble spreads are small in high latitudes.

REFERENCES

Evensen, G., 1994: Sequential data assimilation with a nonlinear quasi-geostrophic model using Monte Carlo methods to forecast error statistics, *J. Geophys. Res*., **99C5**, 10143-10162.

Hunt, B. R., E. Kostelich, and I. Syzunogh, 2007: Efficient data assimilation for spatiotemporal chaos: A local ensemble transform Kalman filter. *Physica D*, **230**, 112-126.

Kalman, R., 1960: A new approach to linear filtering and predicted problems, *J. Basic Eng*., **82**, 35-45.

Liu, H. and X. Zou, 2001: The impact of NORPEX targeted dropsondes on the analysis and 2-3-day forecasts of a landfalling Pacific winter storm using NCEP 3D-Var and 4D-Var systems. *Amer. Meteor. Soc*., **129**, 1987-2004.

Miyoshi, T. and K. Aranami, 2006: Applying a four-dimensional local ensemble transform Kalman filter (4D-LETKF) to the JMA nonhydrostatic model (NHM). *SOLA*, **2**, 128-131.

Miyoshi, T. and S. Yamane, 2007: Local ensemble transform Kalman filterin with an AGCM at T159/L48 resolution. *Mon. Wea. Rev*., **135**, 3841-3861.

Miyoshi, T., S. Yamane, and T. Enomoto, 2007a: The AFES-LETKF experimental ensemble reanalysis: ALERA. *SOLA*, **3**, 45-48.

Miyoshi, T., S. Yamane, and T. Enomoto, 2007b: Localizing the error covariance by physical distances within a local ensemble transform Kalman filter (LETKF). *SOLA*, **3**, 89-92.

Pierre G. and T. Jean-Noël, 2001: Impact of the digital filter as a weak constraint in the preoperational 4D-Var assimilation system of Meteo-France. *Amer. Meteor. Soc*., **129**, 2089-2102.

Parrish, D. F. and J. C. Derber, 1992: The National Meteorological Center's spectral statistical-interpolation analysis system. *Mon. Wea. Rev*., **120**, 1747-1763.

Satoh, M., T. Matsuno, T., H. Tomita, H. Miura, T. Nasuno, S. Iga, 2008: Nonhydrostatic Icosahedral Atmospheric Model (NICAM) for global cloud resolving simulations.
Journal of Computational Physics, the Special Issue on Predicting Weather, Climate and Extreme events, **227**, 3486-3514, doi:10.1016/j.jcp.2007.02.006.

Snyder, C. and F. Zhang 2003: Assimilation of simulated Doppler radar observations with an ensemble Kalman filter. *Mon. Wea. Rev*., **131**, 1663-1677.

Whitaker, J. S. and T. M. Hamill, 2002: Ensemble data assimilation without perturbed observations. *Mon. Wea. Rev*., **130**, 1913-1924.